DOI: 10.1051/epjconf/201714302070

Comparison of FEM calculated heat transfer coefficient in a minichannel using two approaches: Trefftz base functions and ADINA software

Beata Maciejewska[1,*], *Paweł* Łabędzki[1], *Artur* Piasecki[2], *Magdalena* Piasecka[3]

[1]Faculty of Management and Computer Modelling
[2] contractor of the project from the Polish National Science Centre (No. DEC-2013/09/B/ST8/02825)
[3]Faculty of Mechatronics and Mechanical Engineering
Kielce University of Technology, Al. 1000-lecia P.P. 7, 25-314 Kielce, Poland

Abstract. The paper presents the methods of heat transfer coefficient determination for boiling research during FC-72 flow in a minichannel. The boundary condition in the form of distributions of temperature on the outer side of the minichannel heated wall was obtained using infrared thermography. It was assumed two-dimensional steady-state heat flow. The local values of the heat transfer coefficients on the surface between the heated foil and boiling liquid, were determined from the Robin boundary condition. Data necessary for the heat transfer coefficient evaluation were obtained from numerical computations using two approaches: calculation procedure based on the Trefftz functions and FEM simulations by ADINA software. The shape functions were linear combinations of the Trefftz functions. Combinations of the Trefftz functions exactly satisfy the differential equation. Coefficients of the linear combination of the shape function in the approximate solution were chosen to minimize residuals on domain boundary and along common edges of adjacent elements. Temperature measurement points were located in boundary nodes. During FEM simulations 4-node FCBI elements were used, fluid flow was assumed to be laminar, incompressible and material constants of the fluid and of the foil were independent on temperature. The results of the comparative analysis were presented and discussed.

1 Introduction

Recently, there is a demand of using the heat exchangers characterized by small size. At the same time, heat transfer with the change of phase as boiling and condensation processes leads to intensification of resulting in increased efficiency of operation. The problem of heat transfer in heat exchangers with mini spaces was analyzed by a number of researchers. Review of the relevant literature is provided in [1-4] in which the authors presented their investigation results for flow boiling heat transfer in minichannels.

2 Main aim

The main aim of this work is to propose a method of heat transfer coefficient determination for FC-72 flow boiling in a minichannel asymmetrically heated. The boundary condition in the form of distributions of temperature on the outer side of the heated minichannel wall and main thermal and flow parameters are obtained from the experiment. It is assumed two-dimensional steady-state heat flow. The local values of heat transfer coefficients on the surface between the heated foil and boiling liquid were determined from the Robin boundary condition. Data necessary for the heat transfer coefficient evaluation were obtained from numerical computations in which two approaches were used: a calculation procedure based on the Trefftz functions [5-16] and FEM simulations by ADINA software

3 Experimental data

The method of heat transfer coefficient determination is presented for boiling research during FC-72 flow in a rectangular minichannel asymmetrically heated. This minichannel is 1.7 mm deep, 16 mm wide and 180 mm long and is vertically oriented. The measurement module with minichannels is the essential part of the research set up. The schematic diagram of the module is shown in figure 1. The working fluid flowing in the minichannel is FC-72 Flourinert. The heated element is a thin foil (0.1 mm in thickness) made of Haynes-230, which comes into contact with fluid in the minichannel. The temperature of the outer surface of the heated foil was measured with the use of FLIR E60 infrared camera. Thermal accuracy of the camera is ± 1 °C or ± 1% within the temperature range of 0 - 120°C. Example IRT thermogram is shown in the top of the figure 1. Before experiment, the foil was coated with a black paint to

* Corresponding author: beatam@tu.kielce.pl

achieve known emissivity (of 0.83) [2]. It was possible to observe the other side of the foil through a glass pane to visualise the two-phase flow patterns. K-type thermocouples and pressure converters are placed at the inlet and outlet of the measurement module. The experimental data was collected using a data acquisition station and a computer with appropriate software. The research stand was presented in detail in [2].

During experimental series, there is a laminar flow of FC-72 Fluorinert along a minichannel. It is accompanied by a gradual increase in the electric power supplied to the foil followed by an increase in the heat flux transferred to the fluid. Data for the selected setting of the heat flux supplied to the foil during subcooled boiling is analysed. In this boiling region, the liquid flowing in the minichannel was superheated at the interface with the foil and subcooled at the core of the flow. The experimental thermal and flow parameters, physical properties of the heated minichannel wall (made of Haynes-230) and working fluid (FC-72) properties for this setting are presented in Table 1. FC-72 properties were estimated for the average temperature of the fluid (22.5 C) flowing in the minichannel. Thermal conductivity and the other properties of Haynes-230 were taken from the manufacturer data sheet (Haynes Int.) for the average temperature of the heated wall (60 C).

Table 1. Main experimental thermal and flow parameters, physical properties of Haynes-230 and FC-72 properties.

Main thermal and flow experimental parameters	
Heat flux (density)	6 369 kW m^{-2}
Flow velocity	0.15 m s^{-1}
Mass flux	255.3 kg m^{-2} s^{-1}
Reynolds number	1 230 (laminar flow)
Fluid temperature at the inlet	17.8 C
Fluid temperature at the outlet	27.2 C
Pressure at the inlet	112 738 Pa
Pressure at the outlet	102 096 Pa
Inlet liquid subcooling	42.2 C
Physical properties of the heated wall (made of Haynes-230)	
Density	8 970 kg m^{-3}
Thermal conductivity	9.7 W m^{-1} K^{-1}
Specific Heat	397 J kg^{-1} K^{-1}
Physical properties of the working fluid (FC-72)	
Liquid density	1685 kg m^{-3}
Dynamic viscosity	0.0006978 Pa s
Liquid Specific Heat	1044 J kg^{-1} K^{-1}
Liquid Thermal Conductivity	0.0561 W m^{-1} K^{-1}

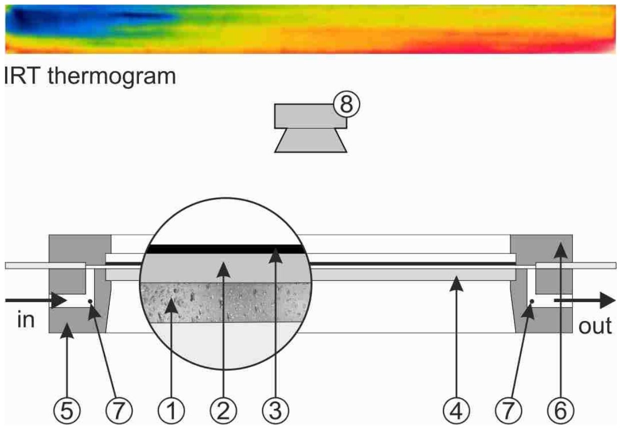

Fig. 1. The schematic diagram of the measurement module: 1-minichannel, 2-heated foil, 3-black paint, 4-glass pane, 5-channel body, 6-front cover, 7-thermocouple, 8-infrared camera.

4 The methods to determine the heat transfer coefficient (FEM)

4.1 The mathematical formulation

The heat flow in the minichannel is assumed to be a two-dimensional steady-state flow. Temperature variability along the minichannel width is not taken into account. The x dimension in the flow direction and the y dimension perpendicular to the flow direction (referring to the thickness of the heated foil) are considered. The local values of heat transfer coefficients are determined from the Robin boundary condition:

$$\alpha(x) = \frac{-\lambda_F \dfrac{\partial T_F(x,\delta_F)}{\partial y}}{T_F(x,\delta_F) - T_f(x,\delta_F + y_i)}, \quad i = 1, 2 \tag{1}$$

where λ_F − the thermal conductivity coefficient of the foil, δ_F − the foil thickness, T_F − the foil temperature, $T_f\,(x, y_i)$ – the fluid temperature at a selected distance from the minichannel depth, calculated in two variants: at 1/4 distance of the minichannel depth from the inner foil surface, $y_1 = d/4$ and at 1/2 distance of the minichannel depth from the foil surface, $y_2 = d/2$, d – the depth of the minichannel (see figure 2).

Those coefficients, on the surface between the heated foil and boiling liquid, are calculated numerically by FEM, with the aid of ADINA software and the calculation procedure based on Trefftz functions.

The following equations are used to describe the boundary-value problem in two adjacent regions:
- Poisson's equation in the heated foil [12]:

$$\nabla^2 T_F = -\frac{I \cdot \Delta U}{A \cdot \delta_F \cdot \lambda_F} \quad \text{for } (x,y) \in \Omega_F \tag{2}$$

- the Fourier–Kirchhoff equation in fluid [16]:

$$\kappa \nabla^2 T_f = w_x(y) \frac{\partial T_f}{\partial x} \text{ for } (x,y) \in \Omega_M \quad (3)$$

The boundary conditions have the form:

$$\frac{\partial T_F}{\partial x}(0,y) = 0 \quad (4)$$

$$\frac{\partial T_F}{\partial x}(L,y) = 0 \quad (5)$$

$$\lambda \frac{\partial T_F}{\partial y}(0,y) = q_{loss} \quad (6)$$

$$T_F(x_p, 0) = T_p \text{ for } p = 1,2,\dots,P \quad (7)$$

$$T_f(x, \delta_F) = T_F(x, \delta_F) \quad (8)$$

$$T_f(0,y) = T_f^{in} \quad (9)$$

$$T_f(L,y) = T_f^{out} \quad (10)$$

$$\lambda_f \frac{\partial T_f}{\partial y}(x, \delta_F + d) = 0 \quad (11)$$

where $\Omega_F = \{(x,y) \in R^2 : 0 < x < L, \ \ 0 < y < \delta_F\}$, $\Omega_M = \{(x,y) \in R^2 : 0 < x < L, \ \ \delta_F < y < \delta_F + d\}$, L – the minichannel length, I − current, ΔU − the voltage drop, A − the surface area of the heated foil determined for IRT, P − the number of measurements obtained from infrared thermography on the outer surface of the heated foil, T_p – the foil temperature measured by infrared thermography at the boundary $y = 0$, q_{loss} − the heat loss to the surroundings calculated as in [2], $w_x(y)$ − component of vector fluid velocity, parallel to the minichannel heated surface [16], λ_F, δ_F, d – defined as for Eq. (1).

4.2 Using the Trefftz functions

To solve the system of equations (2-11), in each element Ω_j, $j = 1, 2, \dots, L1 \cdot L2$ of the domain $\Omega = \Omega_F \cup \Omega_M$, the foil approximate temperature was defined by the formula:

$$T_F^j(x,y) = u(x,y) + \sum_{k=1}^{N} \left(\widehat{T}_F^n - u(x_n, y_n)\right) f_{jk}(x,y) \quad (12)$$

and the fluid approximate temperature was described by the expression:

$$T_f^j(x,y) = \sum_{k=1}^{N} \widehat{T}_f^n g_{jk}(x,y) \quad (13)$$

where: $u(x,y)$ − the particular solution to Eq. (2), $f_{jk}(x,y,)$ – the basis functions determined as linear combinations of the Trefftz functions according to Laplace's equation [9], $g_{jk}(x,y,)$ – the basis functions referred to the Fourier–Kirchhoff equation, $\widehat{T}_F^n$ − the unknown temperature in the n-th node of domain Ω_F, $\widehat{T}_f^n$ − the unknown temperature in the n-th node of domain Ω_M, j − element number, k − basis function number in j-th element, n − node number in the entire domain Ω, N − the number of nodes in the element, $L1$ − the number of elements in the x-axis direction and $L2$ − the number of elements in the y-axis direction.

The basis functions $g_{jk}(x,y,)$ were constructed with the use of the Trefftz functions (that satisfy the Fourier–Kirchhoff equation) given in [16]. The unknown coefficients $\widehat{T}_F^n$ and $\widehat{T}_f^n$ were calculated by minimizing the appropriate functional [2].

4.3 Using the ADINA software

ADINA software in version 9.0 was used for FEM simulations. Two dimensional model of fluid flow was considered. The same boundary conditions as in calculations based on Trefftz functions were used (see equations (4)-(11)). Laminar, incompressible fluid flow was assumed and that material constants of fluid and of the foil were independent on temperature (see Table 1). Under these assumptions FEM model was the same as one represented by equations (2) and (3) [17, section 2.6]. FE mesh is presented on figure 2.

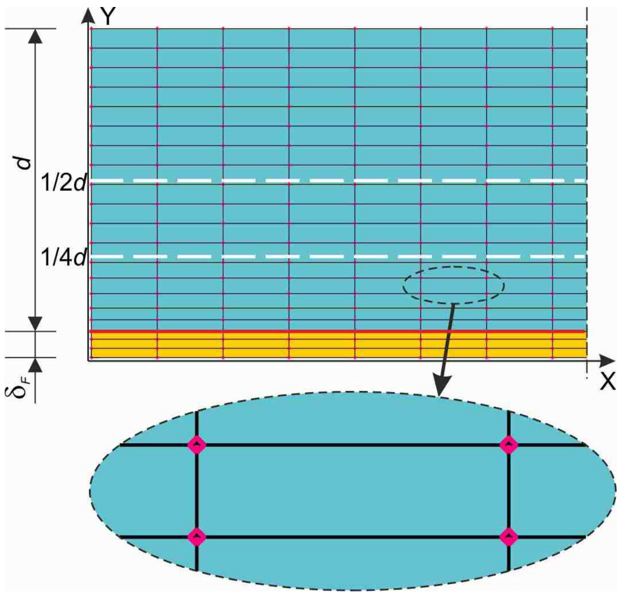

Fig. 2 Scheme of FE mesh fragment (mesh in fluid is coloured in blue, mesh in foil - in yellow).

During simulations 4-node planar FCBI (flow condition-based interpolation) elements were used [17]. Mesh density was established in such a way to decrease mesh quality indicator for heat flux in y direction, which measure jumps of the flux values on adjacent elements, to 10% level (final mesh had 10 000 elements and 10 521 nodes). The temperature was calculated in the nodes, while heat fluxes at the Gauss integration points. Smoothing techniques provided by ADINA were used to obtain flux values in the nodes. As the mesh along that line is sufficiently dense, accuracy of the results remains unaffected.

Temperatures and heat fluxes for the heat transfer coefficient calculation according to Eq. (1) were taken from the FEM calculation, from the lines shown in figure 2 corresponding to: T_F (x, δ_F) - red line (at the foil-fluid boundary), T_f (x, y) - white lines, for the minichannel depths y=d/4 or d/2.

5 Results and discussion

The results are presented graphically in figure 4 as relationship between the heat transfer coefficient and the distance from the minichannel inlet to compare the values calculated using the Trefftz functions (red points) from with that obtained using the ADINA software (green points). Separate plots were generated for two different distances of the minichannel depth: at d/4 distance (figure 3a) and at d/2 distance on the minichannel depth from the foil-fluid boundary (figure 3b), areas of the listed distances are shown in figure 2. The results of the heated surface temperature measurement at the inlet and outlet of a minichannel region (about 10% from each side) could be ignored due to the occurrence of the largest measurement errors when using infrared thermography, as reported in [18]. Additionally, 2D temperature distribution of the heated foil and fluid in the minichannel obtained using the ADINA software was shown in figure 4.

In the subcooled boiling region, the heat transfer coefficient was relatively low. The results obtained using the ADINA software indicate that the local values of the heat transfer coefficient decreased slightly with the distance from the minichannel inlet (figure 4a,b). The highest values of the heat transfer coefficient (above 600 W m^{-2} K^{-1}) are observed very close to the minichannel inlet at the distance 0÷0.0015 m from the channel inlet. The analysis of the data calculated using the Trefftz functions, for channel axis, presented in figure 3b indicates that the heat transfer coefficient in the subcooled boiling region decreased slightly with the distance from the minichannel inlet. The results calculated at the d/4 distance on the minichannel depth from the foil-fluid boundary are higher than those calculated for the d/2 distance and minor data value fluctuations in the range 230÷280 W m^{-2} K^{-1} are observed at the outlet from the minichannel.

Summarizing, in the analyzed boiling region, the heat transfer coefficient calculated using the Trefftz functions did not differ significantly from that obtained using the ADINA software omitting results obtained very close to the minichannel inlet. Too small a number of mesh nodes introduced into the Trefftz functions-based calculation may lead to discrepancies in relation to the results obtained from ADINA. The highest discrepancy, observed at the minichannel inlet, results from the discontinuity of the heated foil temperature field and the mean temperature at the boundary in the fluid in the ADINA model. The boundary conditions used in the calculations should be corrected in both approaches, which would require separating a thermal layer for the calculations and setting in the region the corrected values of the fluid temperature at the channel inlet.

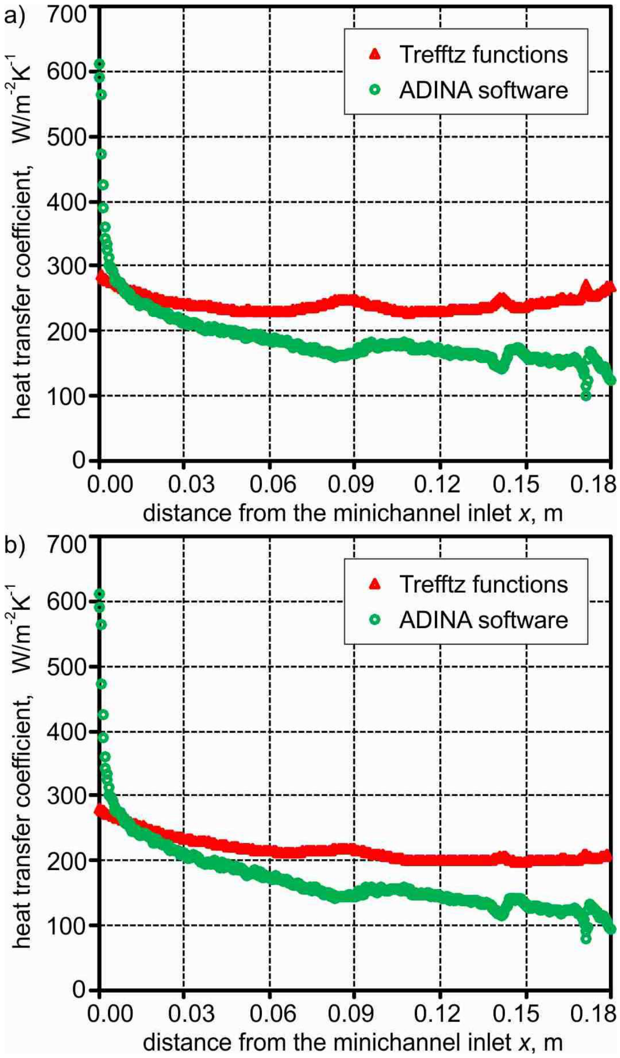

Fig. 3. Heat transfer coefficient vs. the minichannel length, calculated with the aid of Trefftz functions (red points) and obtained by ADINA software (green points), generated at: a) d/4 distance and b) d/2 distance, on the minichannel depth from the foil-fluid boundary.

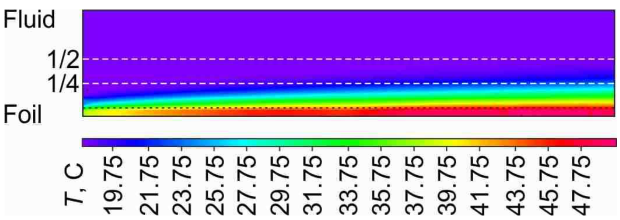

Fig. 4. 2D temperature distributions of the heated foil and fluid in the minichannel obtained using the ADINA software.

6 Conclusions

The results presented in this paper confirm that different FEM methods are suitable for calculations, as verified through experiment. Two methods of heat transfer coefficient determination for the flow boiling of FC-72 in a minichannel were proposed. Data from the experiment were used in the FEM to calculate the heat transfer coefficient in the minichannel using two approaches: Trefftz base functions and ADINA software. The boundary condition in the form of temperature distributions on the outer side of the minichannel heated wall was obtained using infrared thermography. Two-dimensional steady-state heat flow was assumed. The local values of heat transfer coefficients on the surface between the heated foil and boiling liquid were determined from the Robin boundary condition.

The results of the comparative analysis were presented and discussed. In the analysed subcooled boiling region, the heat transfer coefficient calculated using the Trefftz functions did not differ significantly from that obtained using the ADINA software omitting results obtained very close to the minichannel inlet. Boundary conditions near the heated surface at the channel inlet should be adjusted appropriately to improve compatibility of the proposed calculation methods.

ACKNOWLEDGMENTS

The research reported herein was supported in part by a grant from the Polish National Science Centre (No. DEC-2013/09/B/ST8/02825).

References

1. M. Piasecka, B. Maciejewska, Exp. Therm. Fluid Sci. **68**, 459-467 (2015)
2. M. Piasecka, K. Strąk, B. Maciejewska, Heat Transf. Eng. **38** (3), 332-346 (2017)
3. M. Piasecka, Int. J. Refrig. **56**, 198-212 (2015)
4. M. Piasecka, Int. J. Heat Mass Transf. **81**, 114-121 (2015)
5. E. Trefftz, Proc. Int. Kongress für Technische Mechanik, Zürich, 131-137 (1926)
6. I. Herrera, Meth. Partial Diff. Eqs., **16**, 561-580 (2000)
7. K. Grysa, A. Maciąg, A. Pawińska, Int. J. Heat Mass Transf., **55**, 7336–7340 (2012)
8. M. J. Ciałkowski, A. Frąckowiak, J. Therm. Sci., **11**, 148-162 (2002)
9. M. J. Ciałkowski, J. Therm. Sci., **11**, 163-171 (2002)
10. M. J. Ciałkowski, K. Grysa, J. Inv. Ill-Posed Prob., **18**, 595-616 (2010)
11. K. Grysa, B. Maciejewska, J. Theor. Appl. Mech., **51**, 251-264 (2013)
12. S. Hozejowska, R. Kaniowski, M. E. Poniewski, Int. J. Num. Methods Heat Fluid Flow, **24**, 811–824 (2014)
13. A. Maciąg, Int. J. Num. Meth. Biomed. Eng., **27**, 1107-1125 (2011)
14. S. Blasiak, A. Pawinska, Int. J. Heat Mass Transfer, **90**, 710-718 (2015)
15. B. Maciejewska, M. Piasecka, Heat Mass Transfer, DOI 10.1007/s00231-016-1895-1, (2016)
16. S. Hożejowska, J.Theor. Appl. Mech, 53, 969-980 (2015)
17. ADINA CFD & FSI, Raport ARD 13-10, December 2013, ADINA R & D, Inc.
18. M. Piasecka, D. Michalski, K. Strąk, The European Physical Journal Web of Conf. **114**, paper No. 02094 (2015)